Cytoskeletal polymer networks: The molecular structure of cross-linkers determines macroscopic properties

B. Wagner[†], R. Tharmann[†], I. Haase[‡], M. Fischer[‡§], and A. R. Bausch[†¶]

[†]Lehrstühle für Biophysik E22 and [‡]Organische Chemie und Biochemie, Technische Universität München, 80333 Munich, Germany

Edited by Tom C. Lubensky, University of Pennsylvania, Philadelphia, PA, and approved June 14, 2006 (received for review November 24, 2005)

In living cells the mechanical properties of the actin cytoskeleton are defined by the local activation of different actin cross-linking proteins. These proteins consist of actin-binding domains that are separated and geometrically organized by different numbers of rod domains. The detailed molecular structure of the cross-linking molecules determines the structural and mechanical properties of actin networks *in vivo*. In this study, we systematically investigate the impact of the length of the spacing unit between two actin-binding domains on *in vitro* actin networks. Such synthetic cross-linkers reveal that the shorter the constructs are, the greater the elastic modulus changes in the linear response regime. Because the same binding domains are used in all constructs, only the differences in the number of rod domains determine their mechanical effectiveness. Structural rearrangements of the networks show that bundling propensity is highest for the shortest construct. The nonlinear mechanical response is affected by the molecular structure of the cross-linker molecules, and the observed critical strains and fracture stress increase proportional to the length of the spacing unit.

actin cytoskeleton | cross-linking molecules | mechanical properties

For living cells, tight control of the structure and mechanics of their cytoskeleton is crucial for the cells to function properly. The dynamic and local reorganization of one of the major constituents, the actin network, is coordinated by various actin-binding proteins (ABPs). Cross-linking proteins are a major class of ABPs, consisting of actin-binding domains, which are separated and geometrically organized by different numbers of rod domains. Cross-linker molecules vary (*i*) in the type of actin-binding affinity caused by specific binding domains used and (*ii*) in the structure, number, and organization of their spacing rod domains. Both the geometrical structure and actin-binding affinity of ABPs are believed to determine mechanical function *in vivo* (1). Instead of classifying the ABPs by the mechanical function of the cross-linker molecules, the architecture of actin networks is commonly used for a classification of different cross-linking molecules. Whereas very short cross-linkers, such as plastin or fascin, are generally classified as bundling proteins, longer cross-linkers, such as α-actinin or filamin, are thought to induce orthogonal isotropic networks. This qualitative classification does not consider the observed concentration dependence of the structural rearrangements in actin networks (2–4). Different phases, from isotropic cross-linked, composite, or purely bundled networks, have been predicted to occur depending on the interaction potential between rods and the concentrations of linkers and rods (5, 6). Nevertheless, the effect of the structural rearrangements on the mechanical properties of such cross-linked networks is not fully understood. Thus, a correlation of the specific molecular structure of the cross-linker to the resulting network structure and its mechanical response is of great importance. For very rigid cross-linkers, such as scruin, structural rearrangements were successfully related to macroscopic mechanical behavior (7, 8). However, for the biologically important class of compliant cross-linkers, a detailed description is still far from being obtained. Recently, small changes in the molecular structure of human filamins have been shown to especially affect the nonlinear behavior of actin networks (9). For this class of ABPs, (*i*) the number of rod repeats, (*ii*) the rod domain structure, and (*iii*) variable actin-binding affinities are believed to be responsible for the different mechanical properties of the ABPs (1). Although structural arrangements are difficult to quantify, the viscoelastic properties are reliably determinable. The dependence of the elastic moduli on the concentration of cross-linking molecules allows the quantitative characterization of the mechanical effectiveness of different cross-linking molecules. Therefore, the elastic moduli will depend on molecular structure, the binding affinities of the cross-linker, and the resulting structural phases. Consequently, a systematic variation of the molecular structure of cross-linker molecules is needed to correlate the mechanical response of cross-linked networks to the molecular structure of the cross-linkers.

In this work, we relate the geometric structure of different cross-linking molecules with mechanical effectiveness. Synthetic cross-linker molecules based on the naturally occurring *Dictyostelium discoideum* filamin (ddFLN) and hisactophilin (10) are expressed, and the effect on the formation of orthogonal networks and ordered bundles is observed. We demonstrate that the mechanical effectiveness of the different constructs in *in vitro* actin networks depends on the geometrical length of the constructs, respectively on the number of spacing domains.

Results

We analyzed the elastic response and structure of networks, cross-linked by ddFLN (also known as ABP120; GenBank accession no. XP_646669) and compared the obtained results with networks cross-linked by different synthetically constructed cross-linking molecules. For all networks we determined the frequency-dependent elastic modulus G' and the loss modulus, G'' and extracted the quasiplateau modulus ($G_0 = G'$ at 5 mHz) as a function of the molar ratio of cross-linker to actin ($R = c_{\mathrm{xlink}}/c_{\mathrm{actin}}$). The filamin isoform ddFLN is a dimeric molecule, consisting of six tandem repeats of a 100-residue motif (rod domain) with an Ig (IgG) fold and an N-terminal, 250-residue calponin homology domain responsible for actin binding (11, 12). Both chains are arranged in an extended antiparallel fashion interconnecting the two actin-binding domains. The dimerization is mediated by the sixth domain, resulting in an end-to-end distance of $\approx$35 nm (13).

Conflict of interest statement: No conflicts declared.

This paper was submitted directly (Track II) to the PNAS office.

Abbreviations: ddFLN, *Dictyostelium discoideum* filamin; ABP, actin-binding proteins; MW, molecular mass.

[§]To whom correspondence may be sent at the present address: Institut für Biochemie und Lebensmittelchemie, Universität Hamburg, Grindelallee 117, 20146 Hamburg, Germany. E-mail: markus.fischer@chemie.uni-hamburg.de.

[¶]To whom correspondence may be addressed at: Lehrstühl für Biophysik E22, Technische Universität München, James Franck Strasse 1, 85747 Garching, Germany. E-mail: abausch@ph.tum.de.

www.pnas.org/cgi/doi/10.1073/pnas.0510190103

To test how the extended linear geometry influences actin network strength and to systematically relate the molecular structure of different cross-linking molecules to their mechanical effectiveness, we constructed three synthetic chimeric proteins (cross-linkers). In all constructs, hisactophilin was used as the actin-binding domain, and, in two cross-linkers, the length of the spacer region was varied by using different numbers of IgG repeats of ddFLN (see Fig. 2). Depending on the number of rod domains the different constructs were named HisAc-D2-6 (rod repeats 2–6) and HisAc-D5-6 (rod repeats 5 and 6). To investigate a cross-linker without any rod repeat, we constructed a nonspaced, chemically linked head-to-head dimer of hisactophilin, which was designated HisAc-S-S-HisAc.

The junction point between the rod repeat (ddFLN-5) and the hisactophilin moiety in construct HisAc-D5-6 could be easily defined on the basis of the x-ray structure of ddFLN [Protein Data Bank ID code 1WLH (14)], which shows the folding of repeats 4–6. Because of the lack of structural information of the other rod domains of ddFLN, the junction point in construct HisAc-D2-6 had to be determined on the basis of a sequence alignment (see Fig. 5, which is published as supporting information on the PNAS web site).

All constructs were cloned and expressed in *Escherichia coli* cells and purified by Ni-nitrilotriacetic acid affinity chromatography and gel filtration chromatography (*Materials and Methods*; see also *Supporting Materials and Methods* and Tables 1 and 2, which are published as supporting information on the PNAS web site). The purified proteins appeared homogeneous as judged by SDS/PAGE.

The binding properties of these constructs were systematically checked in binding assays with different molar concentrations of cross-linkers compared with actin molecules ($R = c_{\mathrm{xlink}}/c_{\mathrm{actin}}$) spanning more than one order of magnitude (from 0.1 to 1). After centrifugation of those mixtures, all cross-linking constructs were found to be totally incorporated into the actin network as shown by SDS/PAGE (see Fig. 6, which is published as supporting information on the PNAS web site). Thus, all of the cross-linking proteins have been immobilized by binding to the actin network. Consistently, none of the cross-linkers was detected in the supernatant, except when the construct was centrifuged in the absence of actin. Western blot analysis with monoclonal anti-hisactophilin antibodies (15) confirmed these results. These experiments clearly show the similar binding affinities of all three constructs under the experimental conditions.

In addition to our synthetic recombinant constructs, we used the naturally occurring ddFLN in our experiments. Polymerizing actin in the presence of ddFLN resulted in a mainly isotropically cross-linked actin network. Electron micrographs show that, even at high concentrations of ddFLN isotropic networks, only a few embedded bundles are present. The bundles appear loosely packed and significantly curved (Fig. 1*G*). These structural observations depict that the elongated cross-linker ddFLN is rather ineffective in forming strong bundles of actin filaments. Because it is not possible to obtain a reliable quantification of the structural rearrangements from electron micrographs, we determined the mechanical effect of the compliant cross-linker ddFLN on actin networks. In the linear response regime, ddFLN/actin networks show only a weak frequency dependence for the loss (G') and storage (G'') moduli, as can be seen in Fig. 2*D*. The effectiveness of ddFLN in strengthening actin networks was determined by measuring the elastic modulus G_0 at 5 mHz at a given actin concentration ($c_A = 9.5\ \mu$M). Fig. 3 shows that, above a critical concentration of ddFLN ($R^* \approx 0.01 \pm 0.008$), the elastic modulus gently inclined with increasing cross-linker concentration $G_0 \approx R^{0.4\pm0.3}$ (Fig. 3). Accordingly, the ddFLN is not only ineffective at bundling actin filaments but also has only a modest effect on raising the viscoelasticity of these networks.

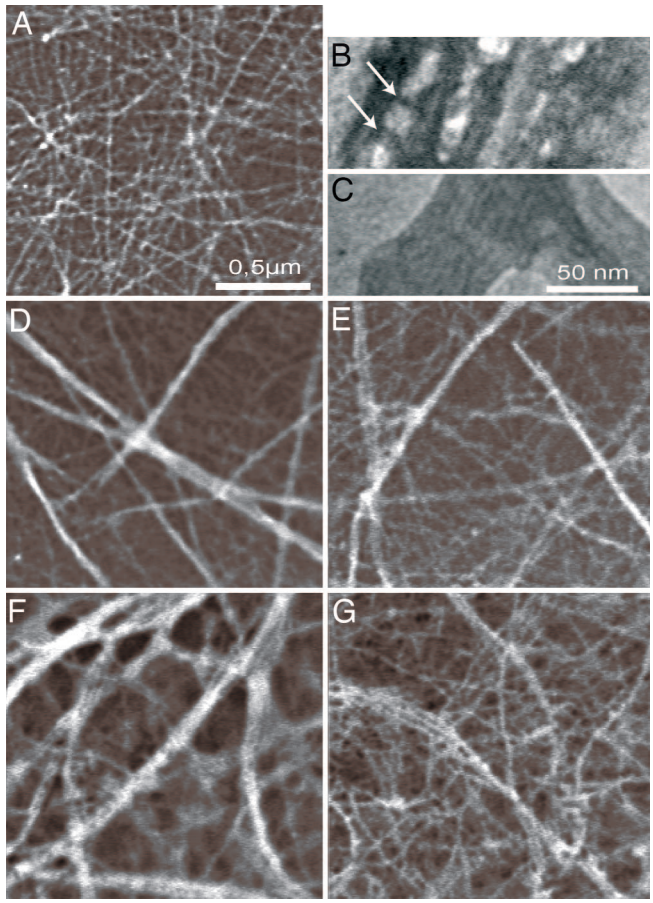

Fig. 1. Transmission electron microscopy images of cross-linked actin networks ($c_A = 9.5\ \mu$M, mean filament length $\langle l_{FA}\rangle = 21\ \mu$m, and $R = 0.1$). (*A*) Actin without cross-linker. (*C* and *D*) HisAc-S-S-HisAc. (*E*) HisAc-D5-6. (*B* and *F*) HisAc-D2-6. (*G*) ddFLN cross-linked actin. Whereas for HisAc-S-S-HisAc the bundles appear straight and compact (*C* and *D*), bundles observed in ddFLN or HisAc-D2-6 cross-linked networks are significantly more curved (*F* and *G*) and appear less dense (*B*, white arrows indicate the cross-linkers). (Magnification: *A* and *D–G*, ×2,950; *B* and *C*, ×28,500.)

The question arises whether these observations can be related to the extended molecular structure of ddFLN.

HisAc-D2-6, which contains rod repeats 2–6 of ddFLN, was the longest synthetic cross-linker protein used in this study. Addition of HisAc-D2-6 cross-linker molecules resulted in an isotropically cross-linked network with curved and widely packed embedded bundles at high concentrations (Fig. 1 *B* and *F*). Furthermore, rheological measurements showed that, below a transition concentration R^*, the mechanical properties of the network are not affected by the addition of the cross-linker. However, above a critical concentration ($R^* \approx 0.0023 \pm 0.0015$), increasing amounts of HisAc-D2-6 resulted in (*i*) an increase of the viscoelastic moduli, (*ii*) a flattening of the frequency dependence of the plateau modulus, and (*iii*) a shift in the crossover frequency (Fig. 2*C*). For all concentrations, the HisAc-D2-6/actin networks are predominantly elastic. As can be seen in Fig. 3, the modest effect of the longest construct on the elastic properties of the network is comparable with that of ddFLN. Again, exceeding a critical concentration, G_0 increases weakly with the concentration of the cross-linker ($G_0 \approx R^{0.5\pm0.2}$). This similarity in mechanical effectiveness is obtained, although the actin-binding domains in ddFLN and HisAc-D2-6 are very different, which suggests that the spacing structure of the cross-linker molecules predominantly determines their mechan-

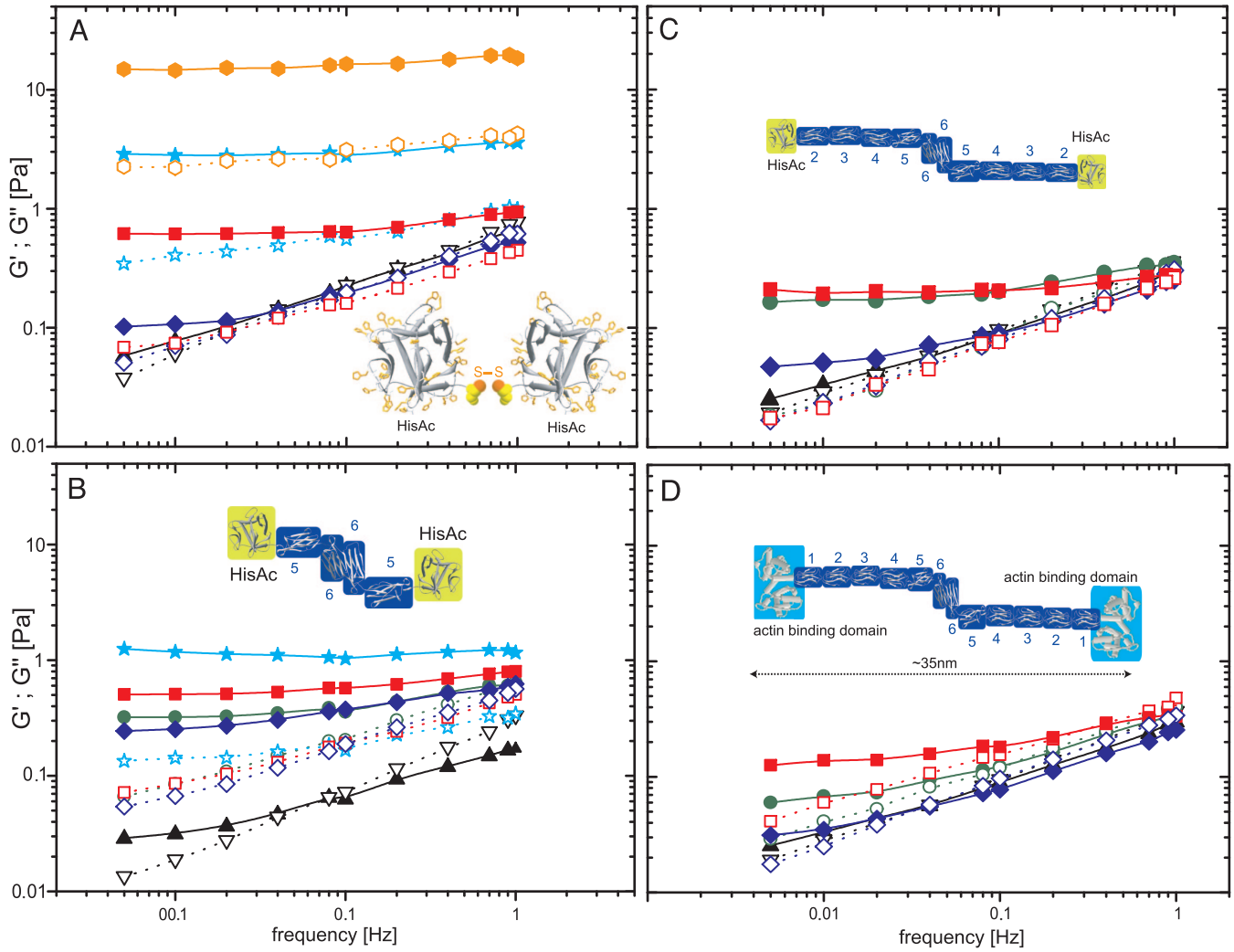

Fig. 2. $G'(f)$ (filled symbols) and $G''(f)$ (open symbols) of cross-linked actin networks measured in bulk with a rotating-disk rheometer at $c_A = 9.5\ \mu$M and $\langle l_{FA} \rangle = 21\ \mu$m at different molar ratios, R. (*A*) HisAc-S-S-HisAc. (*B*) HisAc-D5-6. (*C*) HisAc-D2-6. (*D*) ddFLN. For all cross-linker molecules, the different concentration ratios, R, shown are $R = 0$ (actin; filled triangles and open inverted triangles), $R = 1$ (filled and open orange hexagons), $R = 0.5$ (filled and open stars), $R = 0.1$ (filled and open squares), $R = 0.04$ (filled and open green circles), and $R = 0.02$ (filled and open diamonds). All frequency sweeps show a flattening of G' and a shift in the crossover frequency with increasing R. (*A Inset–D Inset*) Schematics of the cross-linker constructs from structural data of single domains.

ical effectiveness and not the affinity of the actin-binding domain. This result implies that the mechanical effectiveness should be affected by shortening the spacing domains without modifying the binding domains.

Indeed, we observed that a stronger effect on the mechanical properties can be achieved with a decreased number of rod domains. The construct with two rod domains (HisAc-D5-6) already has a significantly stronger effect on the elastic modulus of the network. When the critical concentration ($R^* \approx 0.0015 \pm 0.0005$) is passed, a remarkable increase as a function of cross-linker concentration is observed ($G_0 \approx R^{0.6 \pm 0.1}$) (Fig. 3). For the shortest cross-linker studied, a simple dimer of two hisactophilin molecules chemically fused by a disulfide bridge (HisAc-S-S-HisAc), a high increase in the elastic modulus is observed for $R > 0.01$. Further increase in the cross-linker concentration causes the elastic modulus to change more than two orders of magnitude and scale with $R^{1.2 \pm 0.2}$. Thus, at concentrations above the critical concentration, a clear dependence of the rheological behavior on the number of rod domains can be observed. This increased effectiveness of the shorter constructs in fortifying actin networks can be related to pronounced structural rearrangements. In electron micrographs, a composite network was observed with a significant number of bundles embedded in an isotropic network of filaments above a concentration of $R^* > 0.004$. The number of bundles increases with increasing concentration of the cross-linker molecules, and, at concentrations of $R \geq 0.1$, a percolation of bundles was observed. For HisAc-S-S-HisAc, a pure network of bundles was induced at $R = 1$.

Interestingly, the structure of bundles, as observed by electron microscopy, also was closely related to the structure of the constructs. Whereas the shortest cross-linker induced dense and rather straight bundles, all structures observed after addition of the longest construct or of ddFLN seemed to be significantly bent and appeared fuzzier in the electron microscope pictures (Fig. 1). Below the transition concentration, a purely isotropic network was observed for all constructs studied.

Consequently, the structural rearrangements and the mechanical effectiveness differ significantly between the constructs. The increase of the elastic modulus with increasing concentration of cross-linker molecules ($G_0 \approx R^x$) depends on the molecular mass (MW) and thus on the contour length of the cross-linker constructs. The MW dependence can in first order roughly be approximated by a power law: $x \approx \mathrm{MW}^{-0.7}$. For the threshold value, R^*, no direct dependence was observable.

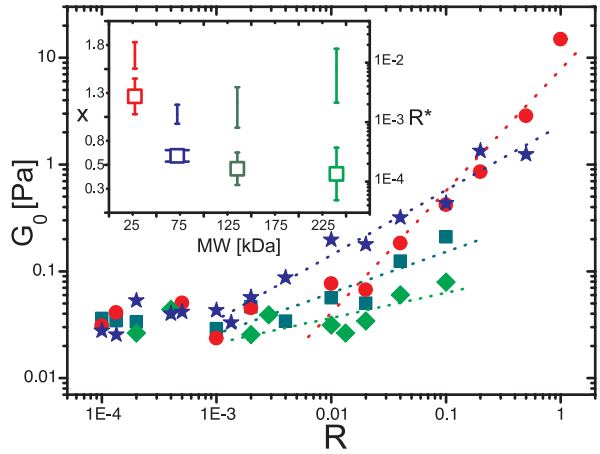

Fig. 3. Plateau modulus G_0 depends on R at $c_A = 9.5\ \mu$M with $\langle l_{FA} \rangle = 21\ \mu$m for HisAc-S-S-HisAc (circles), HisAc-D5-6 (stars), HisAc-D2-6 (squares), and ddFLN (diamonds) cross-linked actin networks. Above a critical ratio R^*, G_0 increases in all cross-linked networks as $G_0 \approx (R)^x$ with $x = 1.2$ (HisAc-S-S-HisAc), $x = 0.6$ (HisAc-D5–6), $x = 0.5$ (HisAc-D2-6), and $x = 0.4$ (ddFLN). (*Inset*) The dependence of the scaling exponent x (squares) and R^* (bars) with cross-linker MW. The error bars were obtained by assuming different threshold values R^* (*Materials and Methods*).

Considering the moderate effect on the linear mechanical response of the actin network, it may be surprising that living cells use ddFLN as a cross-linker. One important aspect could be that cross-linking actin networks by ddFLN adds additional compliances to the network that affect the nonlinear response. Indeed, the nonlinear viscoelastic behavior of the networks depends strongly on the structure of the cross-linking molecules (Fig. 4). For all constructs, the onset of the nonlinear response regime γ_{crit} and the fracture stress τ_{max} was determined at a concentration of $R = 0.1$. As can be seen in Fig. 4, γ_{crit} was observed at increasingly higher strains the longer the construct was. Simultaneously, τ_{max}, the stress at which weakening of the network was observed, depends significantly on the studied constructs. The longest cross-linkers were withstanding the largest stresses, attaining a stress up to 3 ± 0.4 Pa. In contrast, the shortest cross-linker ruptured first, reaching only 0.6 ± 0.3 Pa. Concomitant with the differences in τ_{max} for each cross-linker, the maximal absolute modulus is increased from 1.1 Pa for the shortest cross-linker to 2.2 Pa for HisAc-D5-6 and 4.5 Pa for HisAc-D2-6. The increase of the γ_{crit} and the maximal obtainable modulus depends almost linearly on the MW and thus the contour length of the constructs, as can be seen in Fig. 4.

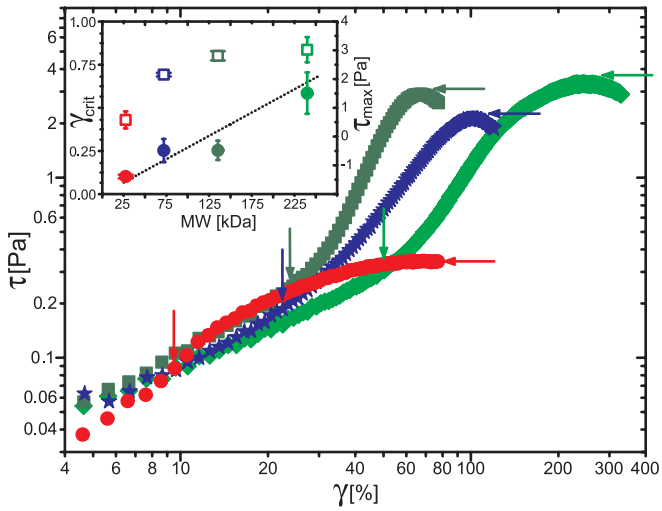

Fig. 4. The recorded stress (τ) and strain (γ) dependence of F-actin networks ($c_A = 9.5\ \mu$M with $\langle l_{FA} \rangle = 21\ \mu$m) with HisAc-S-S-HisAc (circles), HisAc-D5-6 (stars), HisAc-D2-6 (squares), and ddFLN (diamonds) cross-linkers at a constant $R = 0.1$. Arrows pointing left illustrate the maximal reachable stress τ_{max}, and downward-facing arrows indicate the onset of the nonlinearity γ_{crit}. (*Inset*) γ_{crit} (circles) and τ_{max} (squares) are shown over the MW of the cross-linking constructs. The dotted line indicates a linear relation.

Discussion

The systematic variation of the molecular structure of cross-linker molecules shows that the geometry of the cross-linker determines the mechanical network fortification. Short cross-linker constructs result in composite networks in which isolated bundles are embedded in an isotropic network of single filaments. The short cross-linkers are most effective in enhancing the linear viscoelastic properties of actin networks. Longer constructs and ddFLN do not result in a significant increase of the linear elastic moduli, which can be attributed to their lower bundling propensity.

For all cross-linker constructs studied, two regimes were distinguishable in the linear mechanical response: (*i*) one regime with no remarkable increase of the viscoelastic moduli and (*ii*) another regime with an increase of the plateau modulus G_0 correlated with the concentration of cross-linkers. Because the binding affinity is the same for all of the constructs, the differences in the mechanical response of the networks are affected by the number of rod domains and thus the resulting compliance. The structural transition from a weakly isotropically cross-linked network to a strongly isotropically cross-linked network or to a composite network with embedded bundles depends on the geometrical structure of the ABPs. Because of the relatively lower entropic cost associated with cross-linking two filaments, the longer constructs cross-link filaments already at lower concentrations than the shorter constructs but with an impeded bundling efficiency (5). The short-range interaction of shorter constructs results in an increased cooperativity favoring bundling with the transition occurring at higher concentrations. It is important to point out that, although the binding constants of all constructs are kept constant, the molecular structure sensitively affects their effectiveness in bundling, which requires simultaneous binding of both actin-binding domains and therefore may be easiest for the shortest construct.

For the almost covalent and rigid cross-linker scruin, the observed increase of the moduli of $G_0 \approx R^2$ and its observed transition at $R^* = 0.01$ are in excellent agreement with the shortest cross-linker in the present study (8). Depletion forces induce a direct transition from an isotropically cross-linked network to a pure bundle phase, in which the moduli increase as $G_0 \approx R^{3.5}$ (16). These results suggest that the increase of the moduli as a function of concentration in the second regime can be understood as a measure of the bundle propensity that dominates the mechanical effectiveness.

Furthermore, it is important to keep in mind that not only the number of rod repeats but also their structure and the degree of dimerization determine the compliance of a cross-linker molecule. For example, in α-actinin, the spacing domain is composed of four repeats (based on a triple-stranded, coiled-coil α-helix called spectrin domain), which are completely dimerized, resulting in a presumably rigid rod of a contour length of $\approx$36 nm. This cross-linker increases the linear elastic modulus of cross-linked networks quite effectively: $G_0 \approx R^{2.4}$ (3) or $G_0 \approx R^{1.7}$ (17), and, for different long isoforms of α-actinin, significant differences in bundling propensity were observed (18).

In addition, the nonlinear response regime of actin networks is drastically affected by cross-linker proteins (7, 19). Once a critical strain is passed, further increase of the strain on actin/cross-linker

networks results in a stress hardening. Whereas ddFLN cross-linked networks harden by a factor of 10, the shortest cross-linker construct results only in a modest hardening response, almost comparable with pure actin networks, before weakening of the network was observed. The structure of these networks and the increased compliance of the longer cross-linkers allow the network to withstand higher shear stresses. Consistently, the critical strain γ_{crit}, upon which a nonlinear response occurs, is linearly dependent on the MW of the cross-linker constructs (Fig. 4 *Inset*). The fracture stress depends on the force redistribution inside the network, which was observed to depend on the MW and thus the length and compliance of the cross-linkers. Because the binding affinity is kept constant between the constructs, the measured differences have to be attributed to structural differences of the cross-linkers and the resulting networks. Recently, it was shown that a small difference in the molecular structure of human filamin isoforms has significant effects, especially in the nonlinear response of cross-linked networks. Hinged filamins reached fracture stresses of 10–30 Pa, which were 10-fold higher than for nonhinged filamins (9).

For all cross-linker molecules under study, composite network structures were observed in which nonpercolating bundles were integrated in an isotropic network below $R \approx 0.1$. The electron micrographs suggest that the bundle stiffness depends on the cross-linker used, which could be due to the limited number of filaments inside the ddFLN cross-linked bundles or an increased flexibility between the bundled filaments cross-linked by ddFLN or HisAc-D2-6 (20, 21). Therefore, one has to understand how the different compliant bundle structures installed in actin networks affect their mechanical viscoelastic properties. So far, analytical theories fail to describe such composite networks due to the lack of information about the stress distribution over the heterogeneous structural elements (22, 23). Recently introduced mesoscopic simulations of such networks appear to offer the promise of quantitatively describing the underlying physical principles (24, 25).

On the basis of well defined synthetic constructs, we were able to correlate the macroscopic mechanical behavior of cross-linked actin networks with the structure and geometry of actin cross-linking proteins. The observed dependence of the linear elastic properties and the phase behavior on the molecular structure exemplifies how single-molecule properties affect the macroscopic behavior of networks. Because the mechanical properties of the rod domain of ddFLN are well studied (26), such a bottom-up strategy appears to offer the promise of bridging the gap between the understanding of properties of single molecules and complex materials.

Materials and Methods

Actin was prepared from rabbit skeletal muscle according to Spudich and Watt (ref. 27; see also *Supporting Materials and Methods*). All cross-linker constructs were expressed in *E. coli*, and ddFLN was purified from *D. discoideum* cells (see *Supporting Materials and Methods*).

The different cross-linking proteins (ddFLN, HisAc-D2-6, HisAc-D5-6, or HisAc-S-S-HisAc) were added in a molar ratio of cross-linker to actin ($R = c_{xlink}/c_{actin}$) from 1:10,000 to 1:1 before initiating polymerization. All measurements were performed at room temperature (21°C). Samples were gently mixed with pipettes with a cutoff tip. The samples for transmission electron microscopy (EM 400T; Philips, Eindhoven, The Netherlands) were adsorbed (60 s) to glow-discharged, carbon-coated formvar films on copper grids that were washed in a drop of distilled water (60 s) before negative staining (60 s) with 0.8% uranyl acetate. Excess liquid was drained with filter paper to the edge of the grid, which was subsequently permitted to air dry.

The bulk rheological measurements in the linear response regime were performed with a self-built, magnetically driven, rotating-disk rheometer. A sample volume of 400 μl was covered with a phospholipid monolayer of dimystriolphosphatidylcholine dissolved in chloroform to prevent denaturation of actin at the air–water interface. G-actin polymerization was induced by adding 10-fold F-buffer (*Supporting Materials and Methods*), and, after 2 min of gentle mixing, the polymerizing actin was transferred to the sample cuvette and the lipid layer was spread on the surface. After evaporation of the solvent of the lipids for 2 min, the rotating disk was placed onto the sample, and the cuvette was covered with a glass slide to eliminate any evaporation effects. All rheological experiments were performed after 2 h of polymerization at room temperature. We detected the frequency-dependent moduli $G'(f)$ and $G''(f)$ in a frequency range from $f = 1$ Hz to 5 mHz for all samples studied.

To obtain the scaling factor x, it was crucial to determine the threshold concentration of the cross-linkers (R^*), which was done by considering the typically observed measurement error in G_0 of 0.01 Pa, which sets the range of all possible R^*. For this range, a power-law fit was applied to the data, and from all possible slopes the scaling factor x and its error were determined.

The nonlinear regime was probed with a Physica MCR301 (Anton Paar, Graz, Austria) stress-controlled macrorheometer. All measurements were done with plane plate geometry of 50 mm in diameter and gap width of 160 μm at a constant temperature of 21°C. A sample volume of 517 μl was pipetted on the base plate. After polymerizing the sample for 1 h, a constant shear rate ($d\gamma/dt = 12.5\%$ per second) was applied for 40 s while the resulting stress was recorded.

We thank Klaus Kroy and Mark Bathe for many fruitful discussions, M. Rusp for technical assistance in actin purification, and Michael Schleicher (Ludwig-Maximillians University, Munich, Germany) for supplying ddFLN. This work was supported by the Deutsche Forschungsgemeinschaft through Collaborative Research Center 413 TP C3 and by the Fonds der Chemischen Industrie.

1. Wachsstock DH, Schwartz WH, Pollard TD (1993) *Biophys J* 65:205–214.
2. Tseng Y, Fedorov E, McCaffery JM, Almo SC, Wirtz D (2001) *J Mol Biol* 310:351–366.
3. Tempel M, Isenberg G, Sackmann E (1996) *Phys Rev E* 54:1802–1810.
4. Bausch AR, Kroy K (2006) *Nat Phys* 2:231–238.
5. Borukhov L, Bruinsma RF, Gelbart WM, Liu AJ (2005) *Proc Natl Acad Sci USA* 102:3673–3678.
6. Zilman AG, Safran SA (2003) *Europhys Lett* 63:139–145.
7. Gardel ML, Shin JH, MacKintosh FC, Mahadevan L, Matsudaira P, Weitz DA (2004) *Science* 304:1301–1305.
8. Shin JH, Gardel ML, Mahadevan L, Matsudaira P, Weitz DA (2004) *Proc Natl Acad Sci USA* 101:9636–9641.
9. Gardel ML, Nakamura F, Hartwig JH, Crocker JC, Stossel TP, Weitz DA (2006) *Proc Natl Acad Sci USA* 103:1762–1767.
10. Scheel J, Ziegelbauer K, Kupke T, Humbel BM, Noegel AA, Gerisch G, Schleicher M (1989) *J Biol Chem* 264:2832–2839.
11. McCoy AJ, Fucini P, Noegel AA, Stewart M (1999) *Nat Struct Biol* 6:836–841.
12. Stossel TP, Condeelis J, Cooley L, Hartwig JH, Noegel A, Schleicher M, Shapiro SS (2001) *Nat Rev Mol Cell Biol* 2:138–145.
13. Condeelis J, Vahey M, Carboni JM, DeMey J, Ogihara S (1984) *J Cell Biol* 99:119–126.
14. Popowicz GM, Muller R, Noegel AA, Schleicher M, Huber R, Holak TA (2004) *J Mol Biol* 342:1637–1646.
15. Schleicher M, Gerisch G, Isenberg G (1984) *EMBO J* 3:2095–2100.
16. Tharmann R, Claessens MM, Bausch AR (2006) *Biophys J* 90:2622–2627.
17. Tseng Y, Wirtz D (2001) *Biophys J* 81:1643–1656.
18. Meyer R, Aebi U (1990) *J Cell Biol* 110:2013–2024.
19. Xu JY, Tseng Y, Wirtz D (2000) *J Biol Chem* 275:35886–35892.
20. Howard J, Ashmore JF (1986) *Hear Res* 23:93–104.
21. Claessens MM, Bathe M, Frey E, Bausch AR (2006) *Nat Mater*, 10.1038/nmat1718.
22. Heussinger C, Frey E (2006) *Phys Rev Lett* 96:017802.
23. Heussinger C, Frey E (2006) arXiv: cond-mat/0603697.
24. Head DA, Levine AJ, MacKintosh FC (2003) *Phys Rev E* 68:061907.
25. Wilhelm J, Frey E (2003) *Phys Rev Lett* 91:108103.
26. Schwaiger I, Kardinal A, Schleicher M, Noegel AA, Rief M (2004) *Nat Struct Mol Biol* 11:81–85.
27. Spudich JA, Watt S (1971) *J Biol Chem* 246:4866–4871.